Published in final edited form as:
Nat Mater. 2010 September ; 9(9): 768–778. doi:10.1038/nmat2812.

Combinatorial Development of Biomaterials for Clonal Growth of Human Pluripotent Stem Cells

Ying Mei[1,*], **Krishanu Saha**[2,*], **Said R. Bogatyrev**[1], **Jing Yang**[3], **Andrew L. Hook**[3], **Z. Ilke Kalcioglu**[4], **Seung-Woo Cho**[5], **Maisam Mitalipova**[2], **Neena Pyzocha**[2], **Fredrick Rojas**[1], **Krystyn J. Van Vliet**[4], **Martyn C. Davies**[3], **Morgan R. Alexander**[3], **Robert Langer**[1,7,8], **Rudolf Jaenisch**[2,6], and **Daniel G. Anderson**[1,7,8]

[1] Department of Chemical Engineering, Massachusetts Institute of Technology, 77 Massachusetts Avenue, Cambridge, Massachusetts 02139 USA

[2] The Whitehead Institute for Biomedical Research, 9 Cambridge Center, Cambridge, Massachusetts 02142 USA

[3] Laboratory of Biophysics and Surface Analysis, School of Pharmacy, The University of Nottingham, Nottingham, NG7 2RD UK

[4] Department of Material Sciences and Engineering, Massachusetts Institute of Technology, 77 Massachusetts Avenue, Cambridge, Massachusetts 02139 USA

[5] Department of Biotechnology, Yonsei University, Seoul 120-749 Korea

[6] Department of Biology, Massachusetts Institute of Technology, 9 Cambridge Center, Cambridge, Massachusetts 02142 USA

[7] David H. Koch Institute for Integrative Cancer Research, Massachusetts Institute of Technology, 45 Carleton Street, Building E25-342, Cambridge, Massachusetts 02142 USA

[8] Harvard-MIT Division of Health Science Technology, Massachusetts Institute of Technology, 45 Carleton Street, Building E25-342, Cambridge, Massachusetts 02142 USA

Abstract

Both human embryonic stem (hES) cells and induced pluripotent stem (hiPS) cells can self-renew indefinitely in culture, however current methods to clonally grow them are inefficient and poorly-defined for genetic manipulation and therapeutic purposes. Here we develop the first chemically-defined, xeno-free, feeder-free synthetic substrates to support robust self-renewal of fully-dissociated hES and hiPS cells. Materials properties including wettability, surface topography, surface chemistry and indentation elastic modulus of all polymeric substrates were quantified using high-throughput methods to develop structure/function relationships between materials properties and biological performance. These analyses show that optimal hES cell substrates are generated from monomers with high acrylate content, have a moderate wettability, and employ integrin $\alpha_v\beta_3$ and $\alpha_v\beta_5$ engagement with adsorbed vitronectin to promote colony formation. The structure/function methodology employed herein provides a general framework for the combinatorial development of synthetic substrates for stem cell culture.

Correspondence should be addressed to RL (rlanger@mit.edu), RJ (jaenisch@wi.mit.edu), or DGA (dgander@mit.edu).
*These authors (YM and KS) contributed equally to this work.

Author Contributions: All of the authors developed experiments, participated in the generation and analysis of data, and assisted in the writing of the manuscript.

Human pluripotent stem cells (both hES and hiPS cells) hold great promise for regenerative medicine[1-4] and human disease modeling[5]. However, existing methods to grow human pluripotent stem cells are not well suited for genetic manipulation experiments and introduce animal components, increasing the risks of immune rejection. Current methods to grow hES and hiPS cells include growing them on a "feeder" cell layer of mitotically-inactivated mouse embryo fibroblasts (mEFs)[1-3, 6], and on "feeder-free" culture systems, composed of a variety of extracellular matrix (ECM)/serum proteins coated onto tissue culture dishes[7-15] or synthetic materials[16-19] like hyaluronic acid hydrogels. These have been reported to promote hES cell self-renewal when seeded at a suitably high cell density (e.g., ~10^6 cells/ml for the hydrogel)[9, 16, 17] and have not been demonstrated to efficiently promote clonal growth of single hES cells (efficiencies typically <10%). However, gene targeting in pluripotent stem cells necessitates clonal outgrowth of single cells to detect rare targeting events (1 in 10^5-10^6 cells) and requires selective growth of a correctly gene-targeted cell within a population of >10^5 cells.[20-22] Further, current human culture methods utilize either animal products or undefined components, which make it problematic for the potential transplantation applications[4]. Here we employed a high-throughput approach to engineer new culture substrates that could be used to clonally expand human pluripotent stem cells in a chemically-defined, xeno-free, feeder-free manner.

To facilitate rapid synthesis and analysis of synthetic substrates, we manufactured cell-compatible, biomaterial microarrays.[23, 24] Microarrays were prepared from 22 acrylate monomers with diversified hydrophobicity/hydrophilicity and crosslinking densities (Figure 1a). The arrays were prepared by copolymerization between each of 16 "major" monomers (numbered 1 – 16) and each of 6 "minor" monomers (lettered A - F) at six different ratios [100:0, 90:10, 85:15, 80:20, 75:25, 70:30 (v/v)] (Supplementary Figure S1). In this way, arrays with 496 [16 + (16 × 5 × 6)] different combinations were created, comprised of the major monomer (70-100%) and minor monomer (0-30%). These monomer mixtures were robotically deposited in triplicate on a non-cell adhesive layer of poly(hydroxyl ethyl methacrylate) covering conventional glass slides (75 mm × 25 mm), and then polymerized with a long-wave UV source.

We next used fluorescence-activated cell sorting (FACS) of transgenic hES cells to ensure that hES cells were both dissociated with each other and undifferentiated in our assays (Figure 1b). A transgenic green-fluorescent protein (GFP) reporter for Oct4 expression, a marker of pluripotent cells (Supplementary Figure S2), was knocked-in to the BG01 hES cell line and propagated under standard hES cell culture conditions utilizing mEFs.[25] GFP+ sorted hES single cells (Figure 1b, Supplementary Figure S3) were seeded onto the polymer arrays and cultured with mEF-conditioned medium, since soluble growth factors secreted by mEFs help maintain the undifferentiated hES cell state (Supplementary Figure S2c).[7, 17]

Proteins can rapidly adsorb onto the surfaces of materials used for cell culture[26-28]. The surface properties of cell culture substrates can modulate both the amount and the conformation of adsorbed proteins, and thereby interact with cell surface receptors (e.g., integrins) to initiate signal transduction and alter cell behavior.[29] To investigate the potential of different adsorbed proteins, fibronectin, laminin, bovine serum albumin (BSA), and fetal bovine serum (FBS) were separately adsorbed onto the microarrays from solution. In general, FBS was found to most effectively support the propagation of hES cells across the entire array, while fibronectin and laminin coatings led to more differentiation as indicated by down regulation of Oct4-GFP expression (Supplementary Figure 4). Poor cell attachment was observed when arrays were coated with BSA. Therefore, FBS was used initially to coat the polymer array to screen for the suitable polymers ("*hits*") that can support hES cells growth from single cells.

The FBS-coated arrays were seeded at low cell density (40 cells/mm^2), to best model the ability of cells to grow in isolation. Two to ten non-contacting cells were observed on most polymer spots after 24 hrs cell culture (e.g., Figure 2a and Supplementary Figure S5). At various time points during culture, adherent cells were fixed and stained for cell nuclei and two pluripotent stem cell markers, SSEA-4 and Oct4 (Figure 2b). The cellular responses were quantified with laser scanning cytometery.[30] For each polymer, we defined the colony formation *frequency* as the number of polymer spots on which Oct4+ and SSEA-4+ hES cell colonies formed divided by the total number of replicate spots of the same kind of polymer on each array (n=3-18; see Methods). After 7 days of culture, a range of cellular responses was found on the polymer array (Figure 2a): some polymers did not support either survival or growth of dissociated hES cells; some polymers supported the moderate growth of Oct4- differentiating cells; and potential "hit" polymers supported both robust growth and hES cell colony formation (see also Supplementary Figure S6). These differences in cell response demonstrate that polymers can strongly modulate hES cell behavior between days 1 and 7 during colony growth from individual cells.

To better understand the relationship between polymer chemical composition and clonal growth of hES cells, a map of colony formation frequency on the FBS-coated arrays against polymer monomeric composition was generated. In Figure 3a, major monomers were organized in order, from left to right, of increasing colony formation, while minor monomers were organized from bottom to top in order of increasing colony formation. This map indicates that the homopolymer formed from monomer "5" poorly supported clonal growth of hES cells, while most other homopolymers effectively supported cell growth. Tertiary amine containing minor monomer "E" and oligo (ethylene glycol) containing minor monomer "A" negatively influenced colony formation frequency (bottom half of Figure 3a), while minor monomers B, D, and F could robustly support colony formation.

We characterized all polymeric substrates in the library using high-throughput techniques to quantify several materials properties: surface roughness (in air, PBS, and culture medium after FBS adsorption), indentation elastic modulus (in air and fully hydrated in PBS), and surface wettability (Figure 3b-d; Supplementary Figure S7).[31] Surface roughness and elastic properties of bulk material substrata can affect the behavior of adult somatic and stem cells[32-34]. Surface wettability indicating the hydrophobicity/hydrophilicity of polymer surface (quantified as water contact angle, WCA) has been correlated previously with protein adsorption and cell adhesion.[35] To develop quantitative relationships between the colony formation and material properties, we attempted to correlate these properties with colony formation frequency using linear and nonlinear regression (Figure 4, where polymer spots of distinct composition are clustered as a function of the property indicated on each horizontal axis). These data indicate that polymer surface roughness in air (root mean square, RMS~0-25 nm; Supplementary Figure S7a), in PBS (RMS~0-50 nm; Supplementary Figure S7b), and in culture medium after FBS adsorption (RMS~0-110 nm; Figure 4a) did not correlate strongly with colony formation frequency. Standard error of measurement of materials properties was low for replicate samples (e.g., for WCA, <0.9-6.9% in Supplementary Figure S8), such that error bar heights in Figure 4a are indicative of this weak correlation of roughness with colony formation frequency. In contrast, a positive power-law correlation was observed between the indentation elastic modulus E_i of hydrated polymers and colony formation frequency (Figure 4b, inset). However, we note that polymers exhibiting a low indentation elastic modulus (i.e., high elastic compliance) also exhibited a low WCA (Supplementary Figure 9a). Many of these highly compliant polymers contain hydrophilic major monomer 10 and hydrophilic minor monomer A (Supplementary Figure S10a), which is consistent with our observation that the most compliant of these hydrated polymers also exhibited the greatest change in E_i between the dry and fully-hydrated states (Supplementary Figure 9b). This trend is consistent with

previous studies of tissue cell adhesion and proliferation capacity on swellable polymers, where decreased elastic stiffness correlated directly with increased absorption of aqueous solvents.[36] Thus, the power-law correlation between E_i and colony formation frequency (Figure 4b) therefore likely reflects the extent of polymer hydrophobicity/hydrophilicity in the cases where a hydrophilic polymer swells to create a compliant surface (E_i < 0.2 GPa) that poorly supports colony formation. Figure 4b also demonstrates that, for the present array of hydrated polymers, colony formation is not strongly governed by polymer stiffness for E_i of exceeding 0.2 GPa. In contrast, a moderate wettability (WCA~70°) is associated with optimal hES cell colony formation frequency (Figure 4c). A contour projection of colony formation frequency as a function of both E_i and WCA (Figure 4d), shows clearly that the optimum wettability (65° < WCA < 80°) persists over a broad range of polymer stiffness, even for E_i > 200 MPa (3D plot in Supplementary Figure S10b). Thus, together these data indicate that colony formation frequency of hES cells can be modulated most strongly by the wettability of these polymers than by variation in the elastic moduli of these polymers over the range considered.

To further refine our understanding of how this combination of material properties, modulates colony formation, 48 polymers were selected to generate a "secondary" polymer array with 36 replicates. This secondary array was designed to encompass a range of WCA similar to the range in the primary array (Supplementary Figure S11), and the presence of twelve-fold more replicates significantly decreased experimental error. In good agreement with the primary array data, a moderate wettability (WCA~70°) again effectively supported optimal hES cell clonal growth (Supplementary Figure S11-13). Surfaces of all polymers in the secondary array were analyzed using time-of-flight secondary ion mass spectrometry (ToF-SIMS) in a high-throughput manner to provide molecular information of the topmost layers (~10 Å) of each polymer surface.[37, 38] ToF-SIMS spectra from two homopolymers generated from similar monomers 1 and 16 (Figure 5a) were substantially different, suggesting that the polymer surface chemistry cannot be necessarily predicted from the monomer composition alone. Using a chemometric technique (partial least squares (PLS) regression on ToF-SIMS spectra),[31, 38] we correlated surface chemistry contained in the spectra to the colony formation frequency observed on each polymer in the secondary array (Figure 5b). Good agreement between measured colony formation frequency and that predicted from the ToF-SIMS spectra was found (R^2=0.78). Each secondary ToF-SIMS ion associated with functionalities in the polymer structures could be listed with its regression coefficient, "α", a quantitative measure of its contribution to colony formation frequency (Figure 5b and Supplementary Figure S14a). The tertiary amine moiety (characteristic ions $C_3H_8N^+$, $C_2H_6N^+$, CN^-) and tertiary butyl moiety ($C_4H_9^+$) was identified by the PLS analysis to be correlated most strongly with a low colony formation frequency, while hydrocarbon ions ($C_2H_3^+$, $C_3H_3^+$), oxygen containing ions (CHO_2^-, $C_3H_3O^+$, $C_2H_3O^+$) from esters and ions from cyclic structures (C_6H^-, C_4H^-, C_2H^-) had the largest effect on promoting colony formation. The oxygen containing ions and hydrocarbon ions can be attributed to the acrylate groups ($CH_2{=}CHCO_2^-$) in each monomer which form the backbone chain and the pendant ester groups after polymerization. Monomers with di- and tri-acrylates, which contain the most acrylate groups in our library, indeed showed the highest colony formation frequencies.

The refined quantitative relationships among surface chemical structure and hES cell clonal growth generated from the secondary array provides an integrated view of all the cell responses seen on the primary array. On the primary array, the pendent functional groups in mono-acrylates (4, 5, 7, 10) have sizeable effects on colony formation (Figure 3a). For instance, the presence of tertiary butyl, a large non-polar functional group (α<0, Figure 5b), in the major monomer 5 resulted in low colony formation. For most di- and tri-acrylates major monomers (1, 2, 8, 9, 11, 12, 13, 14, and 15) in the primary array, high acrylate

content supported robust clonal formation (Figure 3a) as expected from the large positive α (Figure 5b). The exceptions (3, 6, 16) can be attributed to the presence of a long chain of propylene glycol/ethylene glycol (for glycols, $\alpha<0$, Figure 5b). Although the ethylene glycol moiety can be found in the monomer chemistry of additional di-acrylates major monomers such as 1, 2, 9, 11, ToF-SIMS analysis indicated much higher propylene/ethylene glycol content present at the surface of homopolymers 3, 6, and 16 compared to 1, 2, 9, and 11 (Figure 5a; Supplementary Figure S14b). Further, the PLS model based on the secondary array data was used to predict hES cell colony formation of all 16 homopolymers in the primary array based entirely on their ToF-SIMS spectra (R^2=0.7, Figure 5b). This demonstrates that the model can be used to quantitatively predict hES cells clonal growth on a variety of acrylate polymers outside of the training set of the model.[39]

Since polymers with a moderate WCA generated from multiple acrylate groups performed best in these experiments, we chose homopolymer of monomer 9, a di-acrylate with phenyl groups, and the copolymer with 15-30% monomer A, a tri-acrylate, to further validate the screening results. We fabricated “hit arrays” where the entire polymer array is composed of one “hit” polymer (i.e., 9 or 15A-30%). The colony formation *efficiency* of mEFs and “hit” polymer spots was quantified based on the ratio of hES cells colonies formed on day 7 per attached hES cell on day 1 (Figure 6a). About 20-25% of attached hES cells on day 1 created GFP+, SSEA4+ undifferentiated hES cell colonies after seven days of culture on either the mEFs substrate or on the hit polymers. In contrast, cells on vitronectin- and matrigel-coated tissue culture polystyrene (TCPS) exhibited predominately differentiated growth, had lower Oct4 expression (similar to Figure 2e), and did not form typical hES cell colonies with distinct borders (Figure 2c-d). Further, nearly all (>95%) spots on hit arrays can support the expansion of Oct4+, SSEA4+, Nanog+, and Tra1-60+ cells after 7 day culture from completely dissociated hES single cells (Figure 6b), and similar behavior was seen with other pluripotent cell lines: an hiPS cell line (Supplementary Figure S15a-b) and a non-transgenic hES cell line (Supplementary Figure S15c-d).

The hit arrays were further evaluated for their capacity to maintain pluripotency of hES cells after more than 2 months of culture (>10 passages). Cells after prolonged culture were found to maintain an undifferentiated state with robust expression of hES cell markers, Oct4, Nanog, Tra1-60 and SSEA-4 (as in Figure 6b). Clonal efficiency of cells after long-term culture remained ~20%. In addition, cells could be passaged immediately to mEFs (Supplementary Figure 16a), and such immediate attachment and growth suggests that the hit polymers do not select for a rare subpopulation in parental culture. Additionally, a normal karyotype showed the capacity of both “hit” polymers (9 and 15A-30%) to support genomic stability of hES cells after a long-term culture (Figure 6c). Gene expression results (Figure 6d) confirmed robust differentiation of these hES cells into all three germ lineages after 13 days of embryoid body cultivation, and derivatives of all three embryonic germ layers were seen in teratoma assays (Figure 6e). These results demonstrate that hES cells cultured on the polymeric hits maintain their full pluripotent potential.

To develop a more clinically relevant, defined culture system for hES cells, long-term culture was conducted on human serum (HS) coated “hit” polymer arrays in mTeSR1 medium, a completely chemically defined media (Supplementary Figure S17). HS-coated “hit” polymer arrays supported the expansion of dissociated hES cells in a similar manner to arrays coated with FBS (Figure 6a). Further, the HS-coated hit arrays could support long-term culture for more than 1 month (>5 passages), with robust expression of hES cell markers (Supplementary Figure 16b). Lastly, the HS-coated hit polymers could support the undifferentiated growth of hiPS and other hES cell lines (Supplementary Figure S15).

To investigate the potential pathways through which human serum may be important for colony formation, we performed blocking experiments of several highly-expressed integrins on the hES/hiPS cell surface (Figure 6f). Although there are multiple integrins on the hES cell surface that can interact in a complex manner to promote cell adhesion and self-renewal,[40, 41] blocking the vitronectin-binding integrins, $\alpha_v\beta_3$ and $\alpha_v\beta_5$, resulted in a significant decrease in day 1 cell adhesion, while blocking a matrigel-binding integrin β_1[41] had no effect. Vitronectin is also abundantly present in serum[42], and we tested its capacity to support colony formation when coated on the hit polymers. Similar levels of hES cell adhesion at day 1 were observed on HS-coated and vitronectin-coated "hit" polymers (Figure 6f). Colony formation efficiency at day 7 on FBS/HS coated "hit" polymer arrays was identical to the efficiency on vitronectin-coated "hit" polymers (Figure 6a). The histogram of the cell number on the polymer spots at day 1 (Supplementary Figure S5c) indicated that the majority of colonies formed at day 7 are expanded from a single cell. Although vitronectin-coated TCPS was recently reported to support the culture of hES cells[9], these surfaces were not demonstrated to support hES cell clonal growth, and significant differentiation was observed during clonal growth (e.g., Figure 2d). Our results indicate that the surface chemistry of hit substrates interact with vitronectin, which engages with proper hES cell surface receptors (integrin $\alpha_v\beta_3$ and $\alpha_v\beta_5$), to support the clonal, undifferentiated growth of human pluripotent cells.

The biological activities of polymeric substrates can be controlled by surface properties, which in turn can be determined by chemical moieties present on the polymer surface. However, it may be difficult to quantitatively predict the presence of certain chemical functional groups at the polymer surface from the monomer composition alone, as well as the effects of surface chemistry on biological performance[43]. Here we employed high-throughput materials synthesis and analysis to rapidly establish quantitative models between polymer surface chemical structures and hES cell clonal growth. Utilizing surface chemical structure information of the adsorbed protein layer (e.g., vitronectin) did not result in more predictive models of hES colony formation (Supplementary Figure S18), indicating that ToF-SIMS can resolve surface chemistry differences on polymers leading to colony formation but is less likely to resolve protein structural information leading to colony formation. Our analysis suggests that adsorbed proteins from our initial protein coating (but potentially also from culture media or hES cell secretion) need to interact with the appropriate polymer surface chemistry to be in the proper conformation to optimally promote colony formation. In addition to surface chemistry, which was demonstrated to have a controlling effect on stem cell behavior, the geometry of the spot may influence self-renewal of hES cells as well, potentially by enhancing autocrine or juxtacrine signaling.[44, 45] Lastly, the combination of human vitronectin-coated "hit" polymers and mTeSR1 media provide an attractive platform to develop a fully chemically defined, xeno-free, feeder-free culture system, as the only animal component, BSA from the mTeSR1 medium, can be replaced by human serum albumin. Together, these advances may permit the facile growth of clinically-relevant hES/hiPS cells from fully dissociated single cells, thereby enabling more straightforward genetic manipulation.

Methods

Combinatorial Array Preparation

Polymers were printed in a humid Ar-atmosphere on epoxy monolayer-coated glass slides (Xenopore XENOSLIDE E, Hawthorne, NJ) which were first dip-coated in 4 v/v% poly(hydroxyethyl methacrylate), using modifications of robotic fluid-handling technology as described previously[23]. Spots were polymerized via 10 s exposure to long wave UV (365 nm), dried at <50 mtorr for at least 7 days, and coated with 20% serum or other proteins. See

also supplementary methods and figures S1 and S9a for composition of primary and secondary arrays.

Surface Roughness Measurements

Using an AFM instrument (Digital Instruments Dimensions 3000A) in tapping mode, 5 μm regions of each polymer were measured and the RMS roughness was calculated. See also supplementary methods.

Elastic Modulus Measurements

Using a pendulum-based instrumented nanoindenter (NanoTest, Micro Materials Ltd.), experiments were conducted in ambient air or using a modified platform for *in situ* liquid experiments.[46] Samples were indented with a spherical ruby indenter of radius R=500 μm (n=3 locations for each polymer spot) with loading and unloading rates of 0.5 mN/s, dwell of 10 s and a maximum load of 3 mN or a maximum depth of 600 nm. Loading rates were chosen such that the reduced elastic modulus inferred from indentation could be calculated from the initial unloading slope.[47, 48] Indentation elastic modulus presented in the manuscript was calculated from the measured reduced elastic modulus, assuming a Poisson's ratio of 0.49 for all polymers. See also supplementary methods.

Water Contact Angle Measurements

Measurements were the sessile drop type and performed using ultra-pure water on a Kruss DSA 100 apparatus fitted with a piezo-doser head. See also supplementary methods.

Time of flight secondary ion mass spectroscopy (ToF-SIMS)

A secondary ion mass spectrometer (ION-TOF, IV, UK) was operated using a Bi_3^+ primary ion source at 25 kV and in “bunched mode”. A 1 pA primary ion beam was rastered at an area of 100 ×100 μm. Secondary ions were collected from the same area of each polymer spot on the microarray over 10-second acquisition time. Ion masses were determined using a high-resolution Time-of-Flight analyser, and the typical mass resolution (at m/z 41) was just over 6000.

Cell Culture

hES cell lines BG01 and WIBR3 were maintained on mitomycin C-inactivated mouse embryonic fibroblast feeder (mEFs) layers in standard medium. hES BG01-Oct4-GFP cells were made by introducing a Oct4-GFP-puro construct into hES cells.[25] hiPS C1 cells were derived through lentiviral infection of Oct4, Sox2, and Klf4 and cultured on mEFs as described previously[49]. For EB-induced differentiation, hES cell colonies were cultured for 13 days in nonadherent suspension culture dishes (Corning) in DMEM supplemented with 15% FBS.

For FACS sorting, hES or hiPS cell lines were cultured in 10 μM Rho-associated Kinase (ROCK) inhibitor (Calbiochem; Y-27632) for 24 hr in standard mEF conditions prior to sorting. Cells were harvested enzymatically with 1 mg/ml collagenase and then with 0.05% trypsin for 5 minutes at 37°C. hiPS cells were immunostained using SSEA-4. Cells were collected in media with ROCK inhibitor and sorted on a FACSAria Flow Cytometer (Becton Dickinson, San Jose, CA). Cells were subsequently plated on various surfaces in medium supplemented with ROCK inhibitor for the first 24 hrs of culture to reduce initial apoptosis of completely dissociated hES cells.[50] For HS-coated hit arrays, culturing occurred in mTeSR1 media (Stemcell Technologies). Long-term culture on hit arrays occurred in mTeSR1 media and by passaging 1:3 every 5-7 days using collagenase. See also supplementary methods.

Biological assays

For teratoma formation, hES cells were injected subcutaneously in the back of SCID mice (Taconic) and tumors generally developed within 4-8 weeks. After sectioning, teratomas were diagnosed based on hematoxylin and eosin staining. For karyotype analysis, chromosomal studies were performed by Cell Line Genetics (Madison, WI) using standard protocols for high-resolution G-banding. For immunocytochemistry, cells were fixed in 4% paraformaldehyde in PBS and immunostained according to standard protocols. See also supplementary methods.

Numerical methods

Principal component analysis (PCA) and partial least squares (PLS) regression were carried out using the Eigenvector PLS_Toolbox 3.5 using the SIMPLS algorithm. For linear and nonlinear least-squares regression, Excel (Microsoft) was used. Contour and 3D plots were generated in MATLAB4 (Mathworks) using the v4 griddata method of data interpolation. See also supplementary methods.

Efficiency measurements

Using a low 1.6 cells/mm^2 seeding density, day 1 cell and day 7 colony numbers on mEFs and matrigel were normalized per scanned surface area and on “hit” polymer spots as per “hit” array (1875 mm^2, 1728 replicates). For experiments on TCPS, single cells were sorted individually directly into each well of a coated 96-well plate. Day 1 cell and day 7 colony numbers were measured by manually counting stained wells. For vitronectin-coated, matrigel-coated, and HS-coated TCPS in mEF-conditioned media, no GFP+ colonies were observed: in about 30% of cases we observed only differentiated cell growth. See also supplementary methods.

Supplementary Material

Refer to Web version on PubMed Central for supplementary material.

Acknowledgments

We thank C. Beard, R. Alagappan, P. Xu, P. Wisniewski, C. Araneo, K. Wood, J. Daussman, R. Flannery, D. Fu, E. Luther and Compucyte for technical support. We thank all the members of the Langer lab and Jaenisch lab for helpful discussions and comments on the manuscript. R.J. was supported by NIH grants R37-CA084198, RO1-CA087869, and RO1-HD045022. R.L., R.J. and D.G.A. are advisors to Stemgent and R.L. and R.J. are cofounders of Fate Therapeutics. Financial support for J.Y. is from the Wellcome Trust 085246. K.S. is supported by the Society in Science: The Branco-Weiss Fellowship. D.G.A., R.L. and Y.M. are supported by NIH DE016516.

References

1. Thomson JA, et al. Embryonic stem cell lines derived from human blastocysts. Science. 1998; 282:1145–1147. [PubMed: 9804556]
2. Takahashi K, et al. Induction of pluripotent stem cells from adult human fibroblasts by defined factors. Cell. 2007; 131:861–872. [PubMed: 18035408]
3. Yu J, et al. Induced pluripotent stem cell lines derived from human somatic cells. Science. 2007; 318:1917–1920. [PubMed: 18029452]
4. Daley GQ, Scadden DT. Prospects for stem cell-based therapy. Cell. 2008; 132:544–548. [PubMed: 18295571]
5. Saha K, Jaenisch R. Technical challenges in using human induced pluripotent stem cells to model disease. Cell Stem Cell. 2009; 5:584–595. [PubMed: 19951687]

6. Amit M, et al. Clonally derived human embryonic stem cell lines maintain pluripotency and proliferative potential for prolonged periods of culture. Dev Biol. 2000; 227:271–278. [PubMed: 11071754]
7. Xu C, et al. Feeder-free growth of undifferentiated human embryonic stem cells. Nat Biotechnol. 2001; 19:971–974. [PubMed: 11581665]
8. Stojkovic P, et al. Human-serum matrix supports undifferentiated growth of human embryonic stem cells. Stem Cells. 2005; 23:895–902. [PubMed: 15888688]
9. Braam SR, et al. Recombinant vitronectin is a functionally defined substrate that supports human embryonic stem cell self-renewal via alphavbeta5 integrin. Stem Cells. 2008; 26:2257–2265. [PubMed: 18599809]
10. Li Y, Powell S, Brunette E, Lebkowski J, Mandalam R. Expansion of human embryonic stem cells in defined serum-free medium devoid of animal-derived products. Biotechnol Bioeng. 2005; 91:688–698. [PubMed: 15971228]
11. Amit M, Shariki C, Margulets V, Itskovitz-Eldor J. Feeder layer- and serum-free culture of human embryonic stem cells. Biol Reprod. 2004; 70:837–845. [PubMed: 14627547]
12. Yao S, et al. Long-term self-renewal and directed differentiation of human embryonic stem cells in chemically defined conditions. Proc Natl Acad Sci USA. 2006; 103:6907–6912. [PubMed: 16632596]
13. Ludwig TE, et al. Feeder-independent culture of human embryonic stem cells. Nat Methods. 2006; 3:637–646. [PubMed: 16862139]
14. Ludwig TE, et al. Derivation of human embryonic stem cells in defined conditions. Nature Biotechnology. 2006; 24:185–187.
15. Rodin S, et al. Long-term self-renewal of human pluripotent stem cells on human recombinant laminin-511. Nat Biotechnol. 28:611–615. [PubMed: 20512123]
16. Li YJ, Chung EH, Rodriguez RT, Firpo MT, Healy KE. Hydrogels as artificial matrices for human embryonic stem cell self-renewal. Journal of biomedical materials research Part A. 2006; 79:1–5. [PubMed: 16741988]
17. Gerecht S, et al. Hyaluronic acid hydrogel for controlled self-renewal and differentiation of human embryonic stem cells. Proc Natl Acad Sci U S A. 2007; 104:11298–11303. [PubMed: 17581871]
18. Villa-Diaz LG, et al. Synthetic polymer coatings for long-term growth of human embryonic stem cells. Nat Biotechnol. 28:581–583. [PubMed: 20512122]
19. Melkoumian Z, et al. Synthetic peptide-acrylate surfaces for long-term self-renewal and cardiomyocyte differentiation of human embryonic stem cells. Nat Biotechnol. 28:606–610. [PubMed: 20512120]
20. Zou J, et al. Gene targeting of a disease-related gene in human induced pluripotent stem and embryonic stem cells. Cell Stem Cell. 2009; 5:97–110. [PubMed: 19540188]
21. Hockemeyer D, et al. Efficient targeting of expressed and silent genes in human ESCs and iPSCs using zinc-finger nucleases. Nature Biotechnology. 2009; 27:851–857.
22. Zwaka TP, Thomson JA. Homologous recombination in human embryonic stem cells. Nature Biotechnology. 2003; 21:319–321.
23. Anderson DG, Levenberg S, Langer R. Nanoliter-scale synthesis of arrayed biomaterials and application to human embryonic stem cells. Nat Biotechnol. 2004; 22:863–866. [PubMed: 15195101]
24. Mei Y, et al. Mapping the Interactions among Biomaterials, Adsorbed Proteins, and Human Embryonic Stem Cells. Advanced Materials. 2009; 21:2781–+.
25. Green JJ, et al. Nanoparticles for Gene Transfer to Human Embryonic Stem Cell Colonies. Nano Lett. 2008; 8:3126–3130. [PubMed: 18754690]
26. Tamada Y, Ikada Y. Effect of preadsorbed proteins on cell-adhesion to polymer surfaces. J Colloid Interf Sci. 1993; 155:334–339.
27. Underwood PA, Steele JG, Dalton BA. Effects of polystyrene surface chemistry on the biological activity of solid phase fibronectin and vitronectin, analysed with monoclonal antibodies. Journal of Cell Science. 1993; 104(Pt 3):793–803. [PubMed: 7686170]

28. van Wachem PB, et al. The influence of protein adsorption on interactions of cultured human endothelial cells with polymers. J Biomed Mater Res. 1987; 21:701–718. [PubMed: 2954965]
29. Keselowsky BG, Collard DM, Garcia AJ. Integrin binding specificity regulates biomaterial surface chemistry effects on cell differentiation. Proc Natl Acad Sci U S A. 2005; 102:5953–5957. [PubMed: 15827122]
30. Luther E, Kamentsky L, Henriksen M, Holden E. Next-generation laser scanning cytometry. Cytometry, 4th Edition: New Developments. 2004; 75:185–218.
31. Urquhart AJ, et al. High throughput surface characterisation of a combinatorial material library. Advanced Materials. 2007; 19:2486–+.
32. Lipski AM, et al. Nanoscale engineering of biomaterial surfaces. Advanced Materials. 2007; 19:553–+.
33. Engler AJ, Sen S, Sweeney HL, Discher DE. Matrix elasticity directs stem cell lineage specification. Cell. 2006; 126:677–689. [PubMed: 16923388]
34. Saha K, et al. Substrate modulus directs neural stem cell behavior. Biophys J. 2008; 95:4426–4438. [PubMed: 18658232]
35. Tamada Y, Ikada Y. Effect of Preadsorbed Proteins on Cell-Adhesion to Polymer Surfaces. Journal of Colloid and Interface Science. 1993; 155:334–339.
36. Thompson MT, Berg MC, Tobias IS, Rubner MF, Van Vliet KJ. Tuning compliance of nanoscale polyelectrolyte multilayers to modulate cell adhesion. Biomaterials. 2005; 26:6836–6845. [PubMed: 15972236]
37. Delcorte A, et al. ToF-SIMS study of alternate polyelectrolyte thin films: Chemical surface characterization and molecular secondary ions sampling depth. Surface Science. 1996; 366:149–165.
38. Vickerman, JC. ToF-SIMS: surface analysis by mass spectrometry. IM Publications; Charlton: 2001.
39. Urquhart AJ, et al. TOF-SIMS analysis of a 576 micropatterned copolymer array to reveal surface moieties that control wettability. Analytical Chemistry. 2008; 80:135–142. [PubMed: 18044847]
40. Meng Y, et al. Characterization of integrin engagement during defined human embryonic stem cell culture. The FASEB Journal. 2009:1–10.
41. Rowland TJ, et al. Roles of Integrins in Human Induced Pluripotent Stem Cell Growth on Matrigel and Vitronectin. Stem Cells and Development. 2009
42. Hayman EG, Pierschbacher MD, Ohgren Y, Ruoslahti E. Serum spreading factor (vitronectin) is present at the cell surface and in tissues. Proc Natl Acad Sci USA. 1983; 80:4003–4007. [PubMed: 6191326]
43. Neuss S, et al. Assessment of stem cell/biomaterial combinations for stem cell-based tissue engineering. Biomaterials. 2008; 29:302–313. [PubMed: 17935776]
44. Guilak F, et al. Control of stem cell fate by physical interactions with the extracellular matrix. Cell Stem Cell. 2009; 5:17–26. [PubMed: 19570510]
45. Peerani R, et al. Niche-mediated control of human embryonic stem cell self-renewal and differentiation. EMBO J. 2007; 26:4744–4755. [PubMed: 17948051]
46. Constantinides G, Kalcioglu ZI, McFarland M, Smith JF, Van Vliet KJ. Probing mechanical properties of fully hydrated gels and biological tissues. Journal of biomechanics. 2008; 41:3285–3289. [PubMed: 18922534]
47. Oliver WC, Pharr GM. An improved technique for determining hardness and elastic modulus using load and displacement sensing indentation experiments. Journal of Materials Research. 1992; 7:1565.
48. Cheng YT, Cheng CM. Scaling, dimensional analysis, and indentation measurements. Materials Science and Engineering: R: Reports. 2004; 44:91–149.
49. Hockemeyer D, et al. A drug-inducible system for direct reprogramming of human somatic cells to pluripotency. Cell Stem Cell. 2008; 3:346–353. [PubMed: 18786421]
50. Watanabe K, et al. A ROCK inhibitor permits survival of dissociated human embryonic stem cells. Nat Biotechnol. 2007; 25:681–686. [PubMed: 17529971]

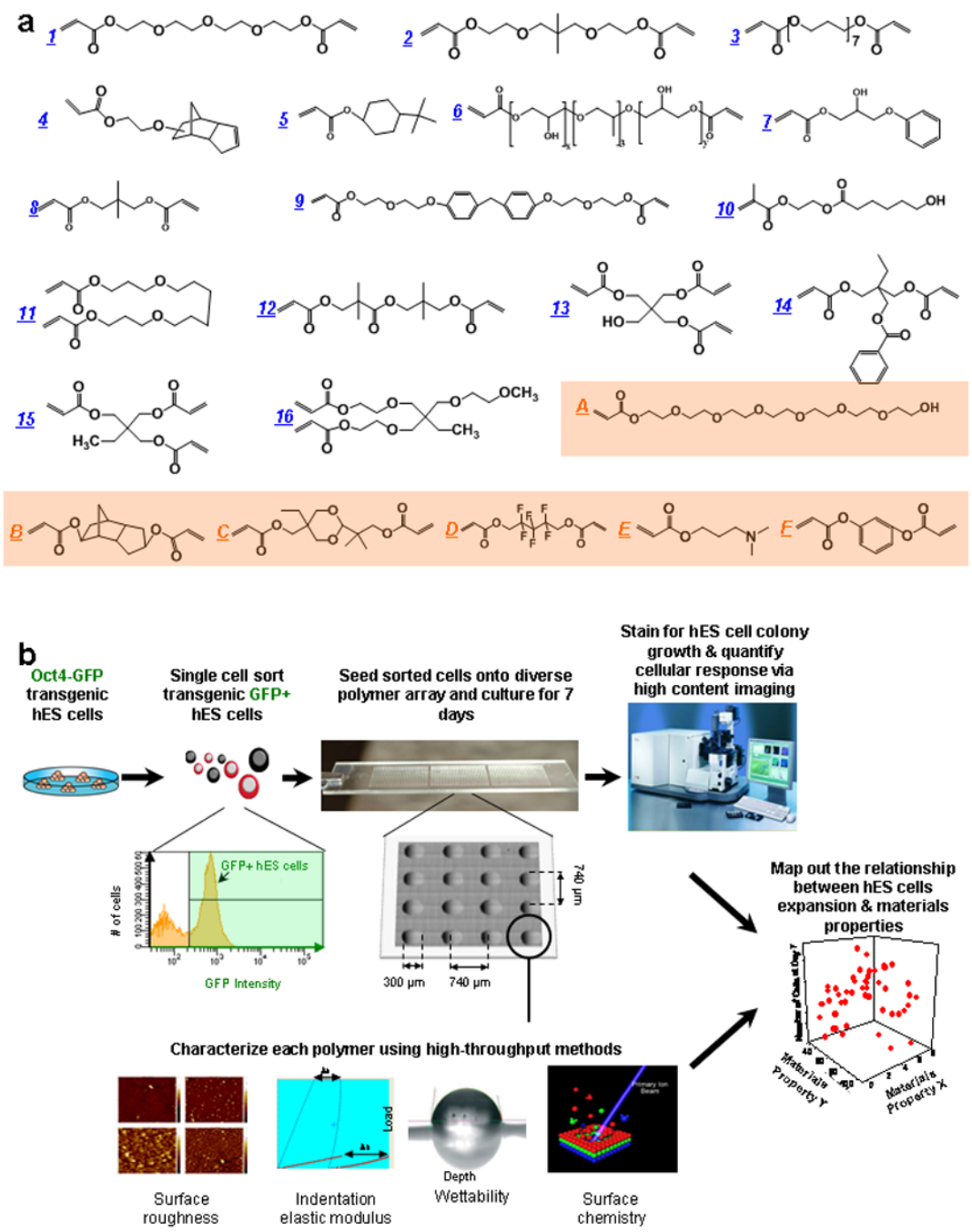

Figure 1. High-throughput screening of biomaterials for clonal growth

a, Monomers used for array synthesis were classified into two categories: “major” monomers that constitute >50% of the reactant mixture and “minor” monomers that constitute <50% of the mixture. Sixteen major monomers were named numerically (blue), and six minor monomers were labeled alphabetically (orange). **b,** Schematic of screen. First, transgenic Oct4-GFP hES cells were maintained on mEFs. Then flow cytometry enabled the isolation of high purity undifferentiated hES cells from the completely dissociated coculture of hES cells and mEFs. A flow cytometry histogram during a representative cell sort is shown. GFP+ cells (right of the black gate) were seeded onto the arrays, while the

differentiated cells and mEFs (GFP-, left of the black gate) were not utilized. A photograph of the polymer microarray with 16 polymer spots is shown to illustrate dimensions and separation. Each polymer was also characterized using high-throughput methods to characterize its surface roughness, indentation elastic modulus, wettability (water contact angle, θ_C) and surface chemistry. Finally, cellular response on polymer array was quantified by using laser-scanning cytometry, and structure-function relationships were determined by numerical analysis of both the cellular response and materials characterization data.

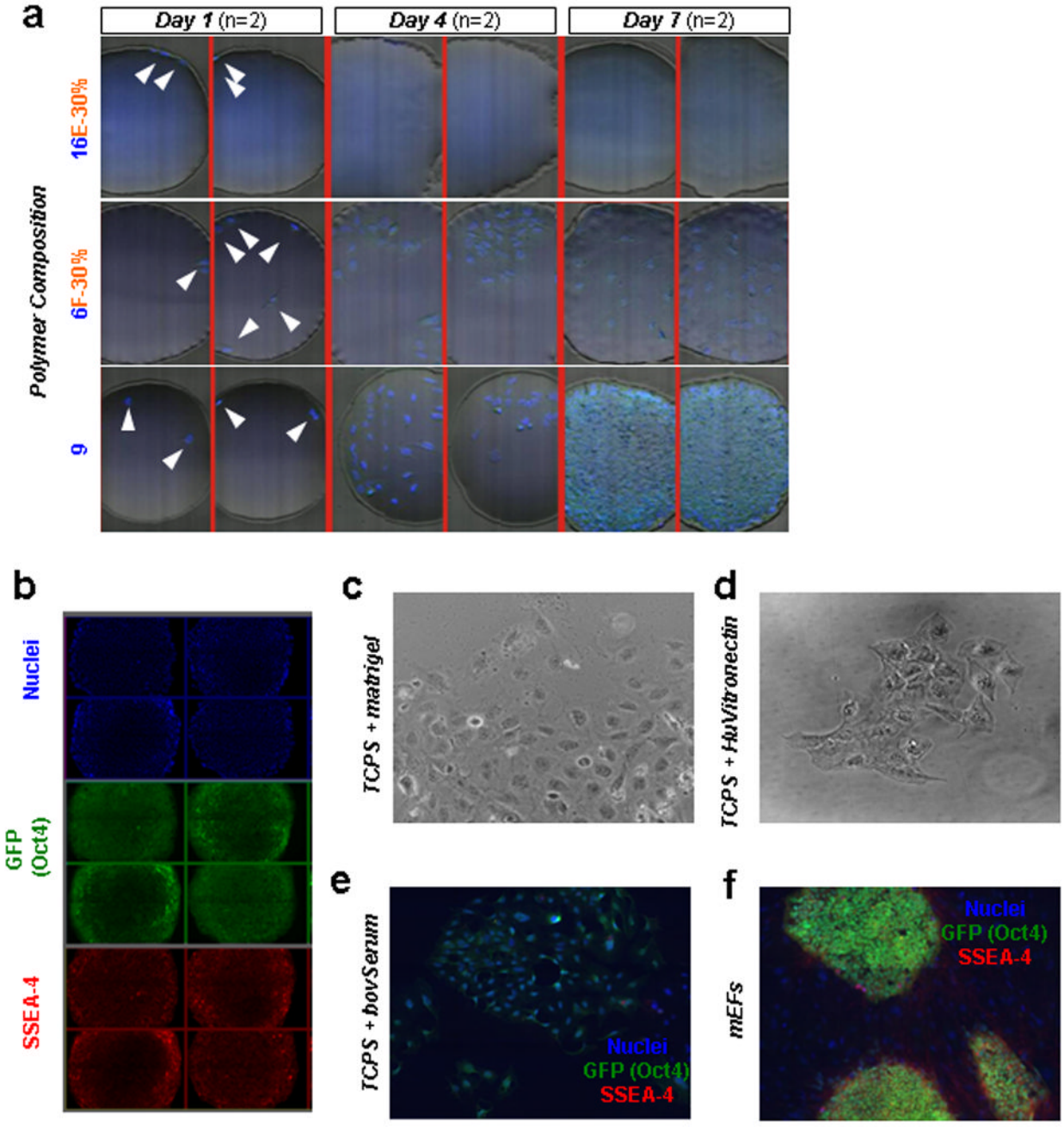

Figure 2. Diverse hES cell behavior on primary polymer arrays

a, Single Oct4-GFP+ hES cells were seeded on the polymer arrays. White arrowheads point to cells attached after one day of culture, indicating a near clonal seeding density for each spot. Diverse cell behavior was seen on the array upon subsequent culture in mEF-conditioned media. Representative images of cell nuclei (stained by Hoechst in blue) on three different polymers (shown are two replicates of each): the 16E-30% polymer did not support either attachment or survival of dissociated hES cells; the 6F-30% supported moderate growth but also differentiation of hES cells; the 9 homopolymer (a “hit” polymer) supported robust growth of hES cells. **b,** Immunostaining of hES cells propagated on “hit” polymer spots for cell nuclei (blue) and for pluripotency markers Oct4 (green) and SSEA4

(red). Due to the raised center of each spot above the plane of the microscope slide, spot centers are not completely in focus, leading to lower intensity at the center of each image. **c-e,** At the near clonal cell densities used for the polymer experiments, hES cells spread out on matrigel-coated tissue culture polystyrene (TCPS), vitronectin-coated TCPS, and bovine serum-coated TCPS substrates in mEF-conditioned media. **f,** In contrast, traditional means of culturing hES cells by using mitotically-inactivated mouse embryonic feeder cells grown on gelatin-coated TCPS ("MEF substrate") could support colony formation at these near clonal cell densities. In e and f, immunostaining was performed for nuclei (blue) and for pluripotency markers Oct4 (green) and SSEA-4 (red). See also Figure 6a for colony formation efficiencies.

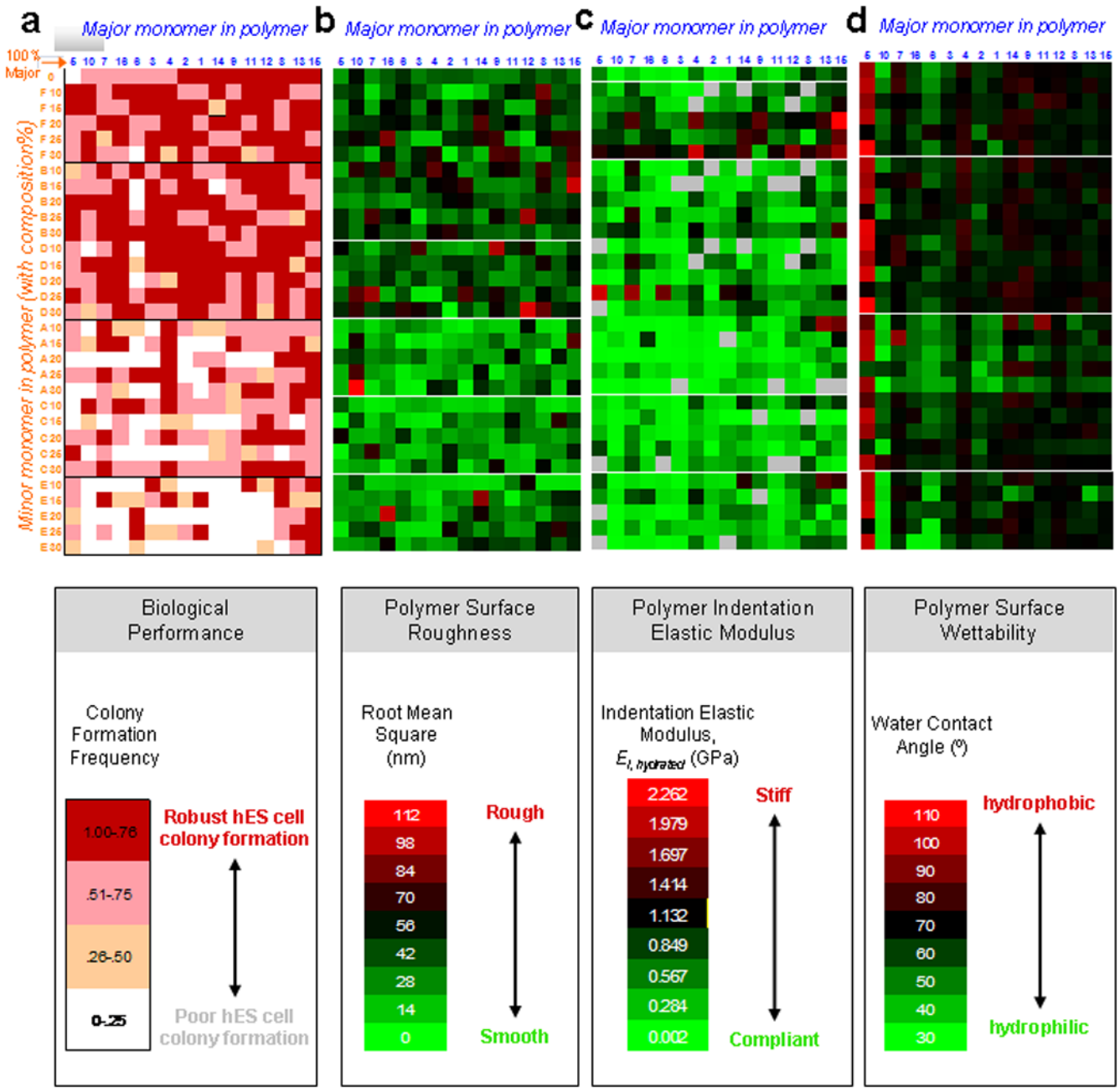

Figure 3. Mapping hES cell behavior to polymer properties using primary arrays

a, Map of hES cell colony formation and polymer composition for all of the 496 monomer combinations in the primary array. For the minor and major composition axes, the numbers and letters indicate the major and minor monomer, respectively, as shown in Figure 1a. Major monomer are listed in order, from left to right, of increasing colony formation, while minor monomers are listed in order of increasing colony formation from bottom to top. Therefore, the region of the map corresponding to highest colony formation is the top right corner, while the region with the lowest is the bottom left corner. Homopolymers are listed at on the upper row. The frequency of colony formation on the primary polymer array was grouped into four categories 0-0.25, 0.25-0.50, 0.50-0.75, and 0.75-1.0 per polymeric spot, as indicated by the intensity of red. **b,** Surface roughness of primary array polymers coated

with FBS in DMEM medium. Map indicating root mean square roughness (see colored legend below) for all of the 496 monomer combinations in the primary array. **c,** Indentation elastic modulus of primary array polymers hydrated in PBS. Map indicating indentation elastic modulus (see colored legend below) for all of the 496 monomer combinations in the primary array. Grey indicates no data obtained. **d,** Wettability of primary array polymers. Map indicating water contact angle (see colored legend below) for all of the 496 monomer combinations in the primary array. Note that polymers in the upper right corner of part *a* with higher colony formation frequencies (dark red) have moderate water contact angles (black) in the upper right corner of part *d*, whereas this region does not correlate to any specific ranges of roughness or elastic modulus in the upper right corner of parts *b* & *c*.

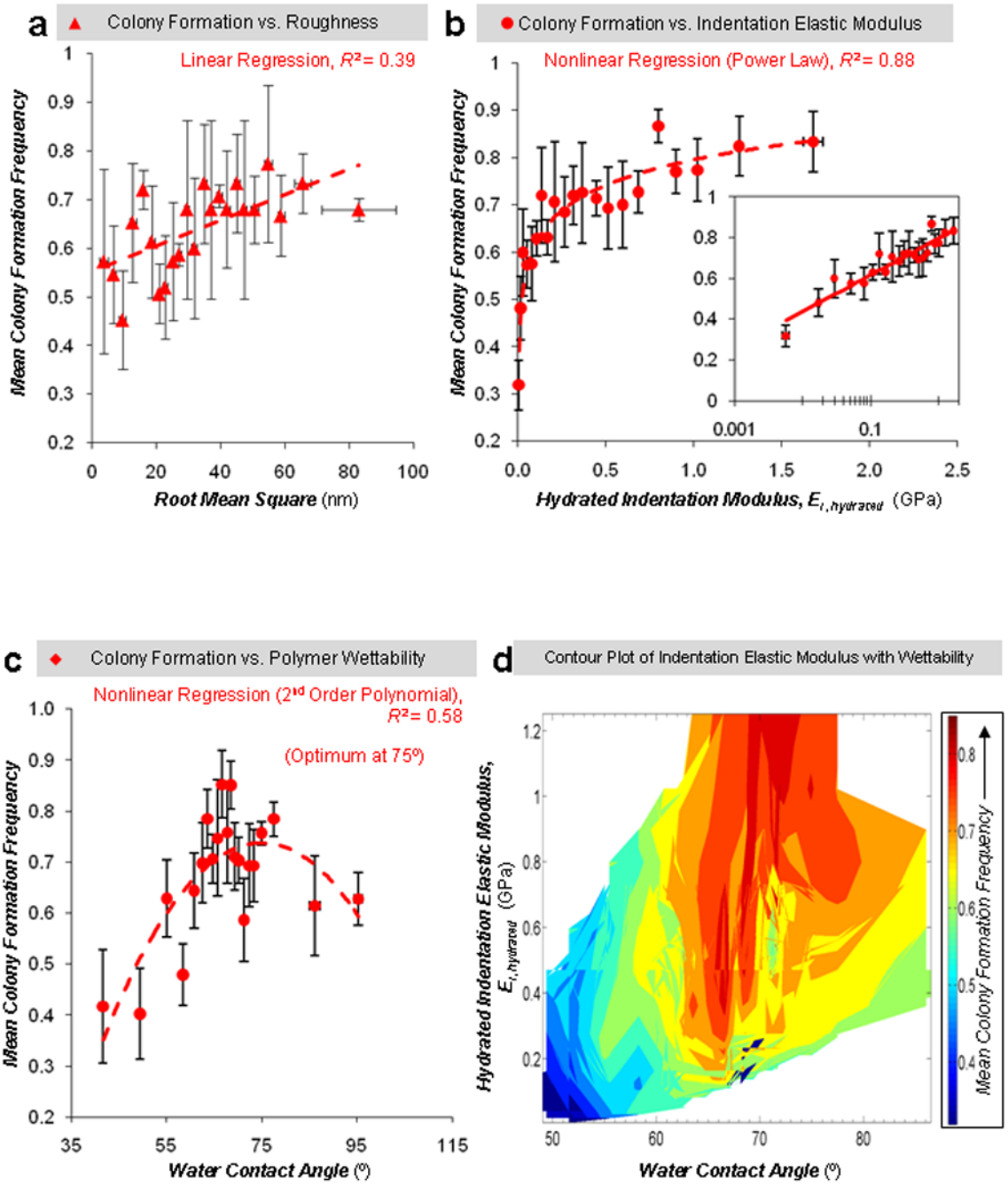

Figure 4. Correlating hES cell behavior to polymer properties using primary arrays

Using data in Figure 3, regression was performed for two properties listed at the top of each plot: colony formation vs. polymer roughness (**a**), colony formation vs. polymer indentation elastic modulus in the hydrated state (**b**), colony formation vs. wettability (**c**), and colony formation as a function of both polymer wettability and indentation elastic modulus in the hydrated state (**d**). After performing linear regression, 2[nd] order polynomial regression, and power law regression, only the regression with the highest R^2 is shown in each plot (dashed line). Insets in parts b are in semi-log format to indicate behavior at low modulus values. Data is sorted into groups of 20-25 spots as a function of increasing WCA, roughness, or

modulus. For contour plot, interpolation between data points (groups of 20-25 spots) was performed on Matlab (see methods). Abscissa error bars represent the standard error of the WCA, roughness, or modulus for a given group of 20-25 spots. In plots a, b, and c, ordinate error bars represent the standard error of the mean of the colony formation frequency of three replicates for a given group.

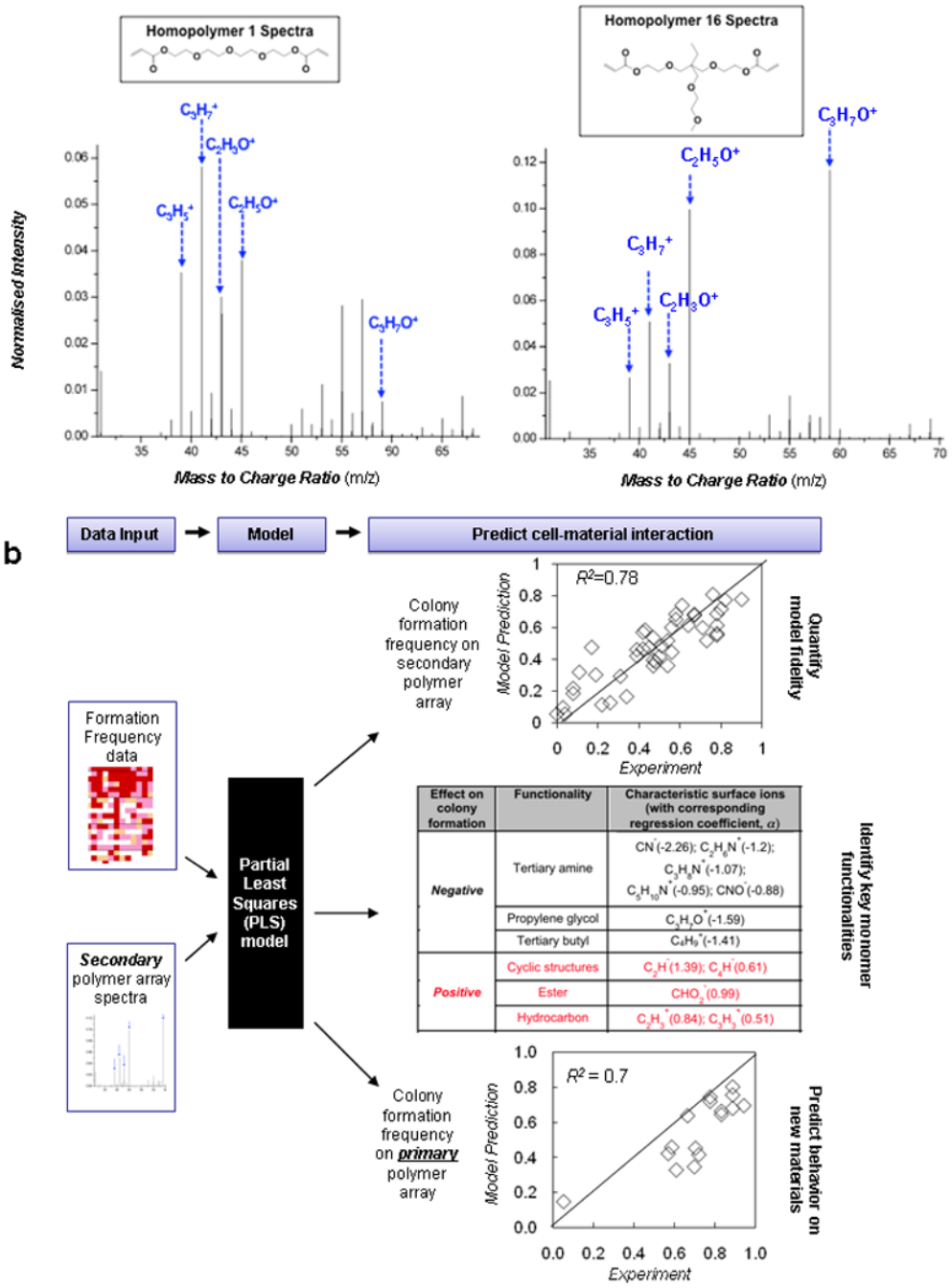

Figure 5. Mapping cell behavior to surface chemistry using secondary arrays

a, ToF-SIMS spectra of homopolymers 1 and 16 indicating that the surface chemistry cannot be necessarily predicted from the monomer chemistry. Arrows delineate higher intensities of hydrocarbon secondary ions ($C_3H_5^+$, $C_3H_7^+$) and ester ions ($C_2H_3O^+$) in the homopolymer 1 spectra. In contrast, higher intensity of ethylene glycol ions ($C_2H_5O^+$) and propylene glycol ions ($C_3H_7O^+$) were observed in the homopolymer 16 spectra. See full analysis of ToF-SIMS spectra in Supplementary Figure S12. **b,** A multivariate partial least squares (PLS) regression method was utilized to quantitatively analyze and predict the cell/materials interactions by correlating ToF-SIMS spectra of polymer spots to their biological

performance (colony formation frequency). The fidelity of PLS models can be quantified by a linear correlation of predicted versus measured colony formation frequency. *Top*: Each spot in the figure represent one of 48 different polymers in the secondary array, and the inserted line represents the ideal situation when prediction match experiments completely. All ions and their regression coefficients, "α", are listed in Supplementary Figure S12a. *Middle table*: Functionalities and their associated characteristic ions supporting or inhibiting hES cell growth. Ions were identified by correlating ToF-SIMS spectra to hES cell growth using PLS regression. Each ion was designated with a regression coefficient, α, that characterizes the relative effect on hES cell colony formation. *Bottom*: As in top plot, but the PLS model was developed on ToF-SIMS spectra from the secondary array (with α's listed in middle table) and was used to predict behavior in the primary array.

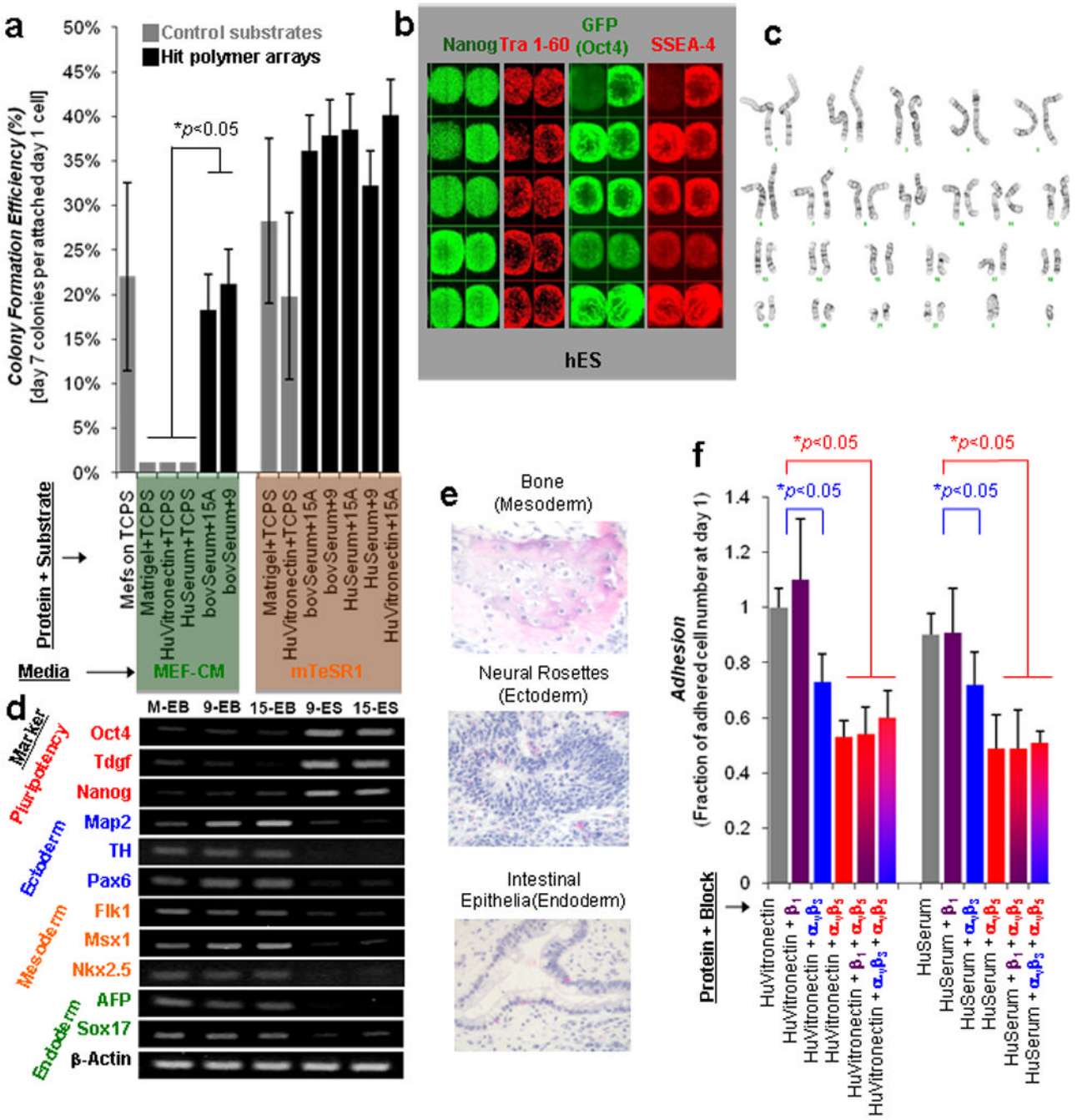

Figure 6. Short- and long-term feeder-free culture on hit polymer arrays

a, Efficiencies of various culture systems to support undifferentiated growth of dissociated hES cells. Two media conditions were used, labeled at the bottom: mEF-conditioned media (MEF-CM) or chemically defined media (mTeSR1). Several combinations of substrate and protein coating were used in conjunction with these media. Three substrates consisted of tissue culture polystyrene (TCPS), hit polymer 9 (“9”; see Figure 1a for monomer structure), and hit polymer 15A-30% (“15A”; see Figure 1a for monomer structures). Four protein coatings consisted of matrigel, bovine serum, human serum, and human vitronectin. Lastly, mEFs on gelatin-coated TCPS in regular hES media was also used. In each condition,

efficiencies were calculated as the number of SSEA-4+ and Oct4+ colonies seen on day 7 normalized to the number of cells attached on day 1. This metric specifically reflects the ability of substrates to promote undifferentiated clonal cell growth after correcting for any differences in initial cell attachment. **b,** Immunostaining of dissociated hES cells propagated on hit FBS-coated "15A-30%" polymer for 7 days against Nanog (green) and Tra-1-60 (red), and on FBS-coated hit "9" polymer for 7 days against Oct4 (green) and SSEA-4 (red). Immunostaining of dissociated hiPS cells propagated on hit "15A-30%" polymer for 7 days; SSEA-4 (red) and cell nuclei (blue). For these studies, hiPS cells were immunostained against SSEA-4, and then the SSEA4+ sorted cell population was used. **c,** Karyotypic analysis of hES cells propagated on hit "9" polymer array for more than 2 months (>10 passages). A normal 46XY karyotype was maintained on the hit array. **d,** Gene expression analyses via RT-PCR of various differentiation markers for the three germ layers generated through embryoid body (EB) *in vitro* differentiation. Lane labels are as follows: "M-EB" for EBs generated from hES cells cultured on mEFs, "9-EB" and "15-EB" for EBs generated from hES cells cultured on 9 and 15A-30% hit polymer arrays respectively, and "9-ES" and "15-ES" for hES cells cultured on 9 and 15A-30% hit polymer arrays respectively. **e,** Teratoma formation in immunodeficient mice by cells cultured on "15A-30%" hit arrays. H&E staining was performed on the teratoma. Resulting teratoma contained tissues representing all three germ layers: ectoderm, epidermal and neural tissue (rosette); mesoderm, bone and cartilage; and endoderm, respiratory epithelium and intestinal-like epithelium. **f,** Fraction of adhered cells after 24 hr of culture in mTeSR1 media on hit polymer arrays coated with either human serum (HuSerum) or human vitronectin (HuVitronectin) and with the specified integrin blocking antibody. Cell number shown here are averages of 24 replicates of the following hit polymers: 15, 15B-10%, 15B-20%, 15B-25%, 15D-10, and 15D-20%. β_1 blocking had minimal effect either alone or in combination with $\alpha_v\beta_5$ and $\alpha_v\beta_3$ blocking, whereas both $\alpha_v\beta_5$ and $\alpha_v\beta_3$ blocking reduced adhesion.